REVISED FIGURES

Figure 1: we added columns with C-isotopes segments proposed in previous papers and revised in this study, and revised the caption accordingly.

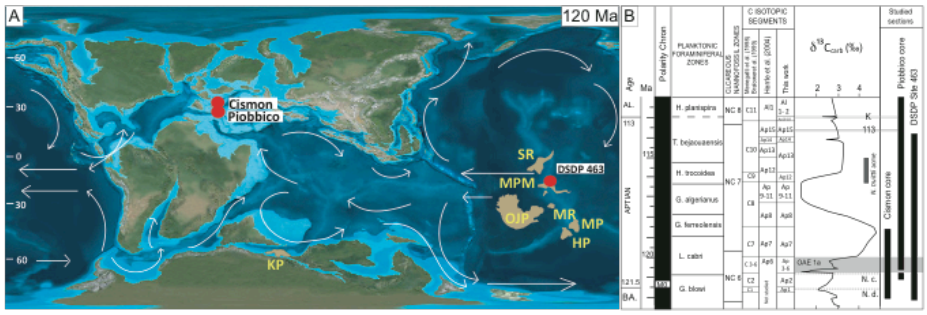

Fig. 1. (A) Location map of studied sites at 120Ma (modified after Erba et al., 2014). OJP=Ontong Java Plateau; KP=Kerguelen Plateau; SR=Shatsky Rise; MPM=Mid-Pacific Mountains; MR=Magellan Rise; MP=Manihiki Plateau; HP=Hikurangi Plateau. **(B)** Stratigraphic ranges of the studied sections. Latest Barremian to earliest Albian chronologic framework is from Erba et al. (2014). Numerical ages are based on the timescale of Malinverno et al. (2012). Codes for C-isotope segments after Menegatti et al. (1998), Bralower et al. (1999), Herrle et al. (2004) and this work are reported. K=Niveau Kilian; 113=113 Level; N.c.=Nannoconid crisis; N.d.=Nannoconid decline.

Figure 2 to 5: as requested, we enlarged font sizes for readability (relative to a "double column page" of CP).

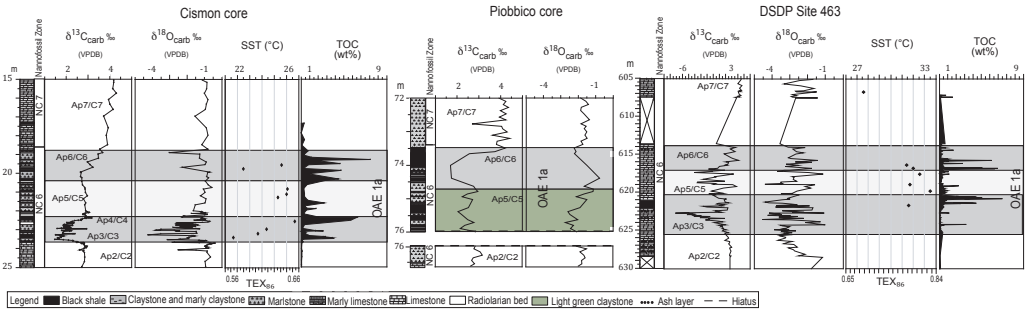

Fig. 2. Correlation between the Cismon core, the Piobbico core and DSDP Site 463. δ13C data after: Erba et al. (1999) and Méhay et al. (2009) for the Cismon core; Erba et al. (2014) for the Piobbico core; Price (2003), Ando et al. (2008) and Bottini et al. (2012) for DSDP Site 463. Bulk δ18O data after: Erba et al. (2010) for the Cismon core; Price (2003), Ando et al. (2008) and this work for DSDP Site 463. TOC after: Erba et al. (1999) and Bottini et al. (2012) for the Cismon core; Ando et al. (2008) for DSDP Site 463. TEX86 after: Schouten et al. (2003) for DSDP Site 463; this work for the Cismon core. For both cores SST was calculated using the equation of Kim et al. (2010). Grey bands indicate intervals of higher (darker) and lower (lighter) TOC values.

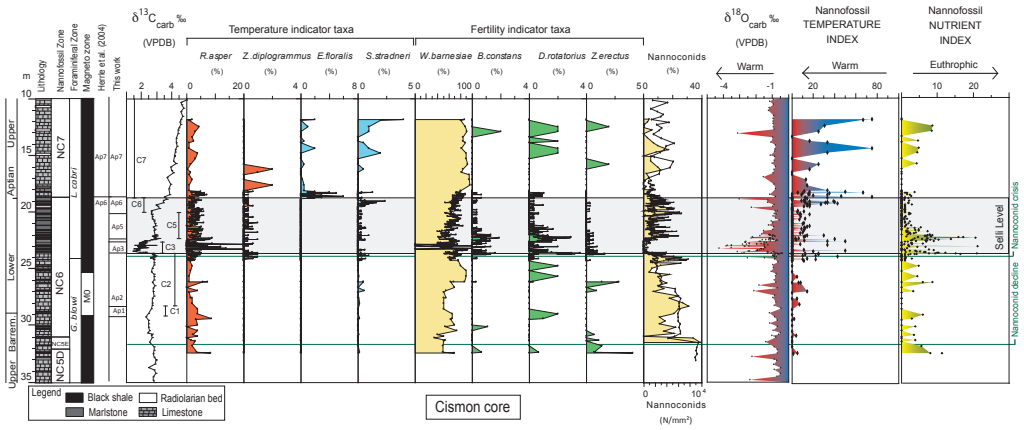

Fig. 3. Cismon core: fluctuations of calcareous nannofossil temperature and fertility indicator taxa. Temperature (TI) and Nutrient (NI) indices based on calcareous nannofossils (low values of the TI indicate high temperatures and vice versa; high values of the NI indicate high surface water productivity and vice versa). δ13C is from Erba et al. (1999) and Méhay et al. (2009). Nannofossil and foraminiferal biostratigraphy is from Erba et al. (1999). Magnetostratigraphy is from Channell et al. (2000). Bulk δ18O data are from Erba et al. (2010).

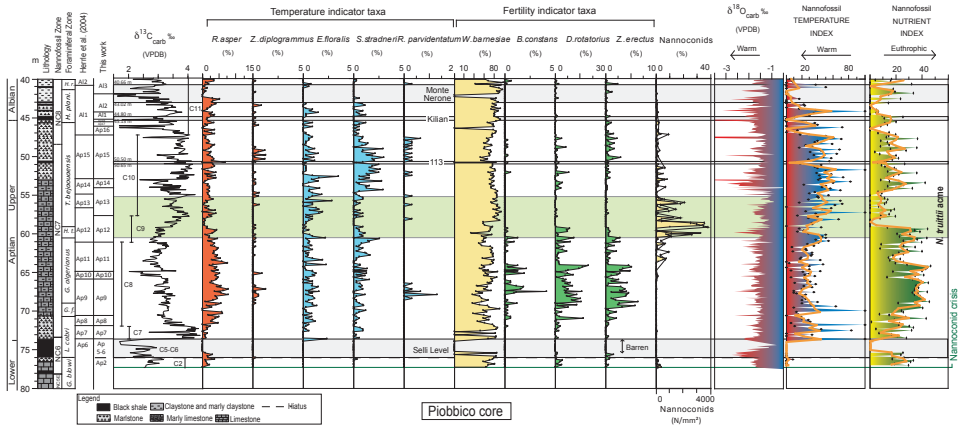

Fig. 4. Piobbico core: fluctuations of calcareous nannofossil temperature and fertility indicator taxa. Temperature (TI) and Nutrient (NI) indices based on calcareous nannofossils (low values of the TI indicate high temperatures and vice versa; high values of the NI indicate high surface water productivity and vice versa). Orange curve indicates smoothed TI and NI records based on three-point moving average. δ13C is from Erba et al. (2014). Nannofossil and foraminiferal biostratigraphy is from Erba et al. (1988) and Tornaghi et al. (1989). Bulk δ18O data are from this work.

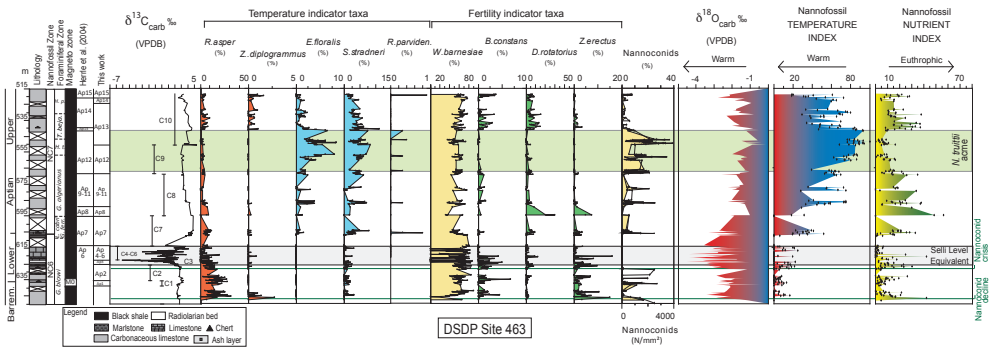

Fig. 5. DSDP Site 463 Mid-Pacific Mountains: fluctuations of calcareous nannofossil temperature and fertility indicator taxa. Temperature (TI) and Nutrient (NI) indices based on calcareous nannofossils

(low values of the TI indicate high temperatures and vice versa; high values of the NI indicate high surface-water productivity and vice versa). δ13C is from Price (2003), Ando et al. (2008), Bottini et al. (2012). Nannofossil and foraminiferal biostratigraphy is from Erba (1994) and Ando et al. (2008). Magnetostratigraphy is from Tarduno et al. (1989). Bulk δ18O data are from Price (2003), Ando et al. (2008), and this work.

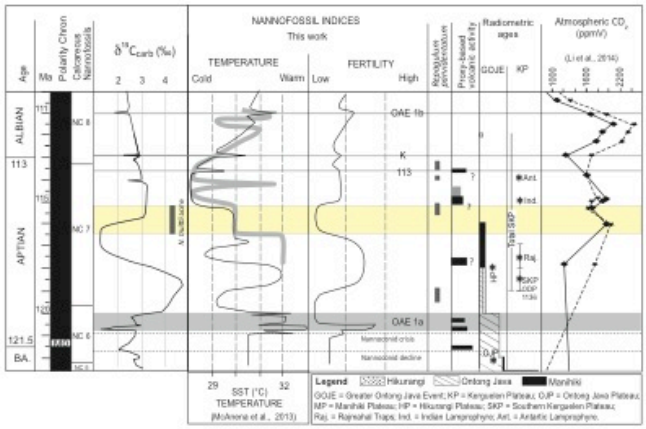

Fig. 7. Composite nannofossil temperature and fertility curves reconstructed for the Aptian including the Aptian/Albian boundary interval (this work) and the earliest Albian (from Tiraboschi et al., 2009). The thick-grey curve represents SST from McAnena et al. (2013). Bio-chemo-magneto stratigraphy after Erba et al. (2014). Numerical ages are based on the timescale of Malinverno et al. (2012). Multiproxy-based volcanic phases and radiometric ages of the Greater Ontong Java Event (GOJE) and Kerguelen Plateau (KP) LIPs are from Erba et al. (2014). Atmospheric CO2: Li et al. (2014).

Figure 8: as requested, we enlarged font sizes for readability (relative to a "double column page" of CP). Also we corrected the Os plot and the position of the CO2-CH4 pulses, because there were some minor graphical mistakes.

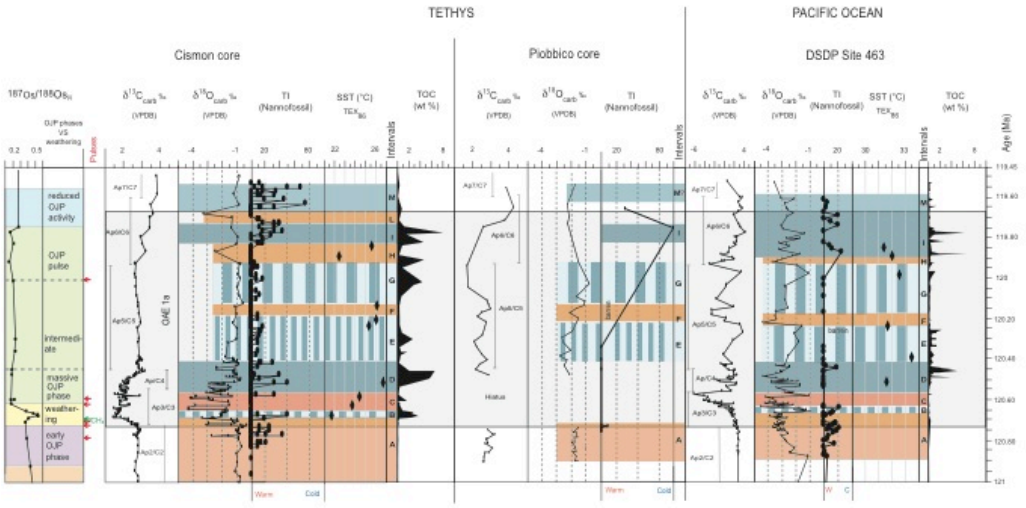

Fig. 8. Nannofossil temperature index (TI), TEX86, and oxygen-isotope values for the Cismon core, Piobbico core and DSDP Site 463 plotted against chemostratigraphy. The age determination is based on the cyclochronology available for the Cismon core (Malinverno et al., 2010). δ13C data after: Erba et al. (1999) and Méhay et al. (2009) for the Cismon core; Erba et al. (2014) for the Piobbico core; Price (2003), Ando et al. (2008) and Bottini et al. (2012) for DSDP Site 463. Bulk δ18O data after:

Erba et al. (2010) for the Cismon core; Price (2003), Ando et al. (2008) and this work for DSDP Site 463. TOC after: Erba et al. (1999) and Bottini et al. (2012) for the Cismon core; Ando et al. (2008) for DSDP Site 463. TEX86 after: Schouten et al. (2003) for DSDP Site 463; this work for the Cismon core (SST calculated using the equation of Kim et al., 2010). On the left is reported the Os-isotope curve (Bottini et al., 2012) and the volcanogenic CO2 pulses (red arrows) reconstructed by Erba et al. (2010). The intervals A to M represent the climatic interludes (warming and cooling) reconstructed in this work.

References

We report below the new references and updates introduced in the revised ms

Bralower, T.J.: Calcareous nannofossil biostratigraphy assemblages of the Cenomanian–Turonian boundary interval: Implications for the origin and timing of oceanic anoxia, Paleoceanography, 3, 275-316, 1988.

Erba, E., Castradori, D., Guasti, G., and Ripepe, M.: Calcareous 4annofossil and Milankovitch cycles: The example of the Albian Gault Clay Formation (southern England), Palaeogeogr. Palaeoclimatol. Palaeoecol., 93, 47–69, 1992.

Erba, E., Bottini, C., Weissert, J.H., and Keller, C.E.: Response to Comment on "Calcareous Nannoplankton Response to Surface-Water Acidification Around Oceanic Anoxic Event 1a", Science, 332, 175, 2011.

Li, X., Jenkyns, H.C., Zhang, C., Wang, Y., Liu, L., and Cao, K.: Carbon isotope signatures of pedogenic carbonates from SE China: rapid atmospheric pCO_2 changes during middle-late Early Cretaceous time. Geol. Mag., 151, in press, doi:10.1017/S0016756813000897, 2014.

Peybernes, C., Giraud, F., Jaillard, E., Robert, E., Masrour, M., Aoutem, M., Içame, N.: Stratigraphic framework and calcareous nannofossil productivity of the Essaouira-Agadir Basin (Morocco) during the Aptian-Early Albian: Comparison with the north-Tethyan margin, Cret. Res., 39, 149-16, 2013.

Thierstein, H.R. and Roth, P.H.: Stable isotopic and carbonate cyclicity in Lower Cretaceous deep-sea sediments: Dominance of diagenetic effects, Mar. Geol., 97, 1 – 34, 1991.

Weissert, H. and Erba, E.: Volcanism, CO2 and palaeoclimate: a Late Jurassic–Early Cretaceous carbon and oxygen isotope record, Journal of the Geological Society of London, 161, 695–702, 2004.